Journal of Catalysis **186,** 470–477 (1999)
Article ID jcat.1999.2590, available online at http://www.idealibrary.com on IDEAL®

The Effect of Particle Size on Aluminosilicate MCM-41 Catalysts Prepared via Grafting Routes

Robert Mokaya

Department of Chemistry, University of Cambridge, Lensfield Road, Cambridge CB2 1EW, United Kingdom

Received April 6, 1999; revised June 4, 1999; accepted June 4, 1999

Aluminosilicate MCM-41 catalysts derived from pure silica materials of varying particle size were prepared via postsynthesis grafting routes. The effect of particle size (which does not change on Al insertion) on the preparation and properties of the Al-grafted materials was studied using a variety of techniques. Particle size has no effect on the uptake and retention of Al (similar Si/Al molar ratios are obtained) but influences the distribution of Al, with larger particles having a higher concentration of surface Al. However, XPS and ^{27}Al MAS NMR studies show that particle size does not radically alter the way in which the surface or bulk Al interacts with the silica framework. Physical characterisation (XRD and N_2 sorption studies) indicates that particle size plays a key role in determining whether or not structural integrity is retained after Al insertion; large-particle pure silica materials, which possess long-range ordering, are more likely to retain their structural ordering and textural properties after Al insertion. The acid content (and therefore proportion of Al sites giving rise to acid sites) is higher in small-particle samples than in large-particle samples. However, particle size has no effect on acid strength. The catalytic activity (for the cracking of cumene) is much higher for small-particle samples; this is presumably due to the higher efficiency with which reactant and product molecules are able to access or exit the shorter pores in small particles as opposed to the much longer (one-dimensional) pores in the larger particles. © 1999 Academic Press

Key Words: **aluminosilicate MCM-41; Al-grafted MCM-41; grafting; particle size; catalytic activity; acidity.**

INTRODUCTION

There is currently great interest in the use of heteroatom-containing mesoporous molecular sieves such as MCM-41 as heterogeneous catalysts (1–3). Heteroatoms may be introduced into mesoporous silicates by direct (mixed-gel) synthesis (4–11) or by postsynthesis grafting methods (12–17). Recently there has been a lot of research effort focusing on the modification of purely siliceous MCM-41, via postsynthesis grafting of heteroatoms, to generate materials with active sites on the inner walls of the well-ordered mesoporous framework (12–17). Grafting of heteroatoms is possible due to the presence, in the amorphous walls of MCM-41, of a high density of silanol groups (18), which can act as anchors for the attachment of guest species via intermolecular condensation. Of particular interest are Al-grafted materials that may be used as solid acid catalysts. Recent studies have shown that the incorporation of Al onto MCM-41 via grafting routes is advantageous with respect to physical characteristics such as structural ordering and stability (16, 17, 19). Furthermore, unlike direct mixed-gel synthesis, grafting allows the preparation of structurally well-ordered, high-Al-content (low Si/Al ratio) materials with the majority of the Al in tetrahedral (framework) positions (12, 13, 16, 17). A further advantage of Al-grafted MCM-41 is higher acid content, which is linked to the presence of easily accessible (acid generating) Al sites on the pore walls rather than buried in the framework as is the case for direct mixed-gel Al-MCM-41 (16, 17).

The aim of this study was to find out the effect of particle size on the preparation and properties of Al-grafted mesoporous aluminosilicates. Due to the advantages it provides, grafting is likely to become an important route for the preparation of mesoporous aluminosilicates derived not only from MCM-41 but also from other forms of mesoporous silicas (such as MCM-48, KIT-1, SBA-*n*, and MSU-*n* silicas) that possess amorphous walls. From a synthesis point of view, particle size is expected to be a crucial factor given that in the grafting procedure the Al is first in contact with the outer surface of the particle before being distributed into the bulk. Therefore the uptake and distribution of Al may be influenced by the particle size of the parent purely sliceous MCM-41. Furthermore since particle size is not altered during grafting it is possible to investigate its effect on acid content and catalytic activity by simply comparing Al-grafted materials prepared from pure silica samples of varying particle size. It is generally accepted that for catalysis, small particle size (and therefore short pore channels that allow easy access of the reactant molecules to the acid sites and diffusion of product molecules out of the pores) is desirable. This is especially relevant for MCM-41 catalysts due to their one-dimensional pore structure in which large particle (or crystallite) size and long-range structural ordering may mean extremely long one-dimensional pores, which may cause diffusion and

0021-9517/99 $30.00

accessibility problems. It is therefore of interest to find out whether particle size exerts any influence on the catalytic activity of MCM-41 catalysts even though they possess pores of diameter much larger than the size of most reactant and product molecules. Presented here are results on the chemical composition, structural ordering, porosity, acidity, and catalytic activity of Al-grafted materials that differ in their particle size.

METHODS

Materials

Synthesis of starting purely siliceous materials. Three purely siliceous MCM-41 materials of varying particle size were used, i.e., (i) a room-temperature-synthesized small crystallite sample designated Si-MCM(S) and (ii) hydrothermally synthesised medium crystallite MCM-41, designated Si-MCM(M) and a larger crystallite sample designated Si-MCM(L).

Si-MCM(S) was prepared by adding tetramethylammonium hydroxide (TMAOH) and sodium hydroxide (NaOH) to an aqueous solution of hexadecyltrimethylammonium chloride (CTACl) of appropriate concentration and stirring for 10 min. Tetraethyl orthosilicate (TEOS) was then combined with the resulting solution at room temperature under stirring. The resulting gel of molar composition TEOS : 0.24 NaOH : 0.12 TMAOH : 112 H_2O : 0.24 CTACl was left to react for 24 h at room temperature. The solid product was obtained by filtration, washed with distilled water, dried in air at 120°C, and finally calcined in air at 550°C for 16 h.

Si-MCM(M) was prepared as follows: tetramethylammonium hydroxide (TMAOH) and cetyltrimethyammonium bromide (CTAB) were dissolved in distilled water by stirring at 35°C. The silica source, fumed silica (sigma), was added to the solution under stirring for 1 h. After further stirring for 1 h the resulting synthetic gel of composition SiO_2 : 0.25 CTAB : 0.2 TMAOH : 40 H_2O was left to age for 20 h at room temperature, following which the gel was transferred to a Teflon-lined autoclave and heated at 125°C for 40 h. The solid product was obtained by filtration, washed with distilled water, dried in air at room temperature, and calcined in air at 550°C for 8 h.

The preparation of Si-MCM(L) was similar to that of Si-MCM(M) except that the hydrothermal crystallisation was performed at 150°C for 48 h.

Grafting of aluminium. Al-grafted MCM-41 materials were prepared at a target bulk Si/Al ratio of 10 (though the concentration of Al in the grafting reagents was kept relatively low) via an aqueous or a nonaqueous method. In the aqueous method 1.0 g of the calcined purely siliceous Si-MCM(X) was added to a 50-ml solution of 0.12 mol L^{-1} (wrt Al) aluminium chlorohydrate (ACH) at 80°C and stirred for 2 h (at 80°C). The resulting solid was obtained by filtration and thoroughly washed with distilled water (until free of Cl^- ions), dried at room temperature, and calcined in air at 550°C for 4 h. The resulting Al-grafted samples were designated ACH10(X), where X is S, M, or L for small, medium, or large crystallite. In the nonaqueous method 2.0 g of calcined purely siliceous material was dispersed in 50 ml dry hexane and added to 150 ml dry hexane containing the appropriate amount of aluminium isopropoxide (AlP) to give a Si/Al ratio of 10. The grafting gel mixture was stirred for 10 min and allowed to react at room temperature for 24 h. The resulting powder was obtained by filtration, washed with dry hexane, dried at room temperature, and calcined in air at 550°C for 4 h to obtain the Al-grafted samples. Two Al-grafted samples, designated AlP10(X), where X is S or L for small or large crystallite, were prepared.

Characterisation

Elemental compositions were determined by X-ray fluorescence. Powder X-ray diffraction (XRD) patterns were recorded using a Philips 1710 powder diffractometer with Cu$K\alpha$ radiation (40 kV, 40 mA), 0.02° step size, and 1-s step time. Textural properties (surface area and pore volume) were determined at −196°C using nitrogen in a conventional volumetric technique by a Micromeritics ASAP 2400 sorptometer. Before analysis the calcined samples were oven-dried at 120°C and evacuated overnight at 180°C under vacuum. ^{27}Al magic-angle-spinning (MAS) NMR spectra were recorded at 9.4 T using a Chemagnetics CMX-400 spectrometer with zirconia rotors 4 mm in diameter spun at 8 kHz. The spectra were measured at 104.3 MHz with 0.3-s recycle delays and corrected by subtracting the spectrum of the empty MAS rotor. External $Al(H_2O)_6^{3+}$ was used as a reference. To ensure quantitative reliability all calcined samples were fully hydrated and equilibrated with room air prior to the measurements (20, 21). X-ray photoelectron spectroscopy (XPS) data were recorded on a VG Scientific photoelectron spectrometer using Al$K\alpha_{1,2}$ radiation (1486.8 eV) from an X-ray source operating at 13 kV and 10 mA. Working pressure was kept below 2×10^{-8} Torr. The spectra were recorded at a photoelectron take-off angle of 45°. Binding energies were referenced to the C 1*s* peak from adventitious carbon surface deposit at 284.8 eV. Data processing details were as given in Ref. (22). SEM images were recorded using a Jeol JSM-820 scanning electron microscope operating at an accelerating voltage of 10 kV. Samples were mounted using a conductive carbon double-sided sticky tape. A thin (ca. 10 nm) coating of gold sputter was deposited onto the samples to reduce the effects of charging.

Acidity Measurements

The acidity was measured using thermally programmed desorption of cyclohexylamine (23–25). The method involved thermogravimetric analysis (TGA) following

adsorption of the base on the catalysts and the number of acid sites capable of interacting with the base after heat treatment at either 80 or 250°C was determined. Freshly calcined samples were exposed to liquid cyclohexylamine at room temperature after which they were kept overnight (at room temperature) and then in an oven at 80°C for 2 h so as to allow the base to permeate the samples. The oven temperature was then raised to 250°C and maintained at that temperature for 2 h. Thermal treatment at 250°C removed the base from the weaker acid sites and was therefore performed so as to determine the population of medium and strong acid sites. Prior to analysis the samples were cooled under dry nitrogen. TGA curves were then obtained for the cyclohexylamine containing samples (thermally pretreated at either 80 or 250°C) using a Polymer Laboratories TG analyser with a heating rate of 20°C/min under nitrogen flow of 25 ml/min. The weight loss associated with desorption of the base from acid sites occurred between 280 and 450°C. This weight loss was used to quantify the acid content (in μmoles of cyclohexylamine per gram of sample), assuming that each mole of cyclohexylamine corresponds to 1 mol of protons (23–25).

Catalytic Testing

The conversion of cumene was performed using a tubular stainless steel, continuous flow fixed-bed microreactor system with helium (25 ml/min) as carrier gas at 300°C and WHSV of 5.5. The catalyst bed (100 mg; 30–60 mesh) was first activated for 1.5 h at 500°C under helium (25 ml/min). For the reaction a stream of cumene vapour in helium was generated using a saturator. The reaction products were separated and analysed using a Carlo Erba HRGC 5300 gas chromatograph on line with the microreactor. Gas chromatographs were obtained automatically on samples of the product stream, which were collected at regular intervals using a Valco 6-port valve. The gas chromatographs were used to calculate the percentage overall (and rate of) cumene conversion.

RESULTS AND DISCUSSION

Starting Pure Silica Materials

Powder X-ray diffraction and scanning electron microscopy (SEM) were used to confirm that the starting pure silica materials used had different particle sizes. The XRD patterns for the three purely siliceous materials are shown in Fig. 1a. The pattern for the room-temperature-synthesized Si-MCM(S) is typical of a material with short- to medium-range hexagonal ordering (26). The relatively low intensity of the (100) diffraction peak along with the large full width at half-maxima (FWHM) and the very low intensity and poor resolution of higher order peaks is indicative of a relatively small coherent scattering domain (CSD) size and therefore a small particle size. The pattern for sample Si-MCM(M) shows higher intensities and better resolved higher order peaks, which are an indication of a larger crystallite size and better long-range ordering than those for Si-MCM(S). The pattern for sample Si-MCM(L), which shows an intense (100) diffraction peak and some well-resolved higher order peaks, is characteristic of a material with large CSD size and good long-range ordering. The differences in particle size indicated by the XRD results were confirmed by the SEM micrographs in Fig. 2, which clearly show large variations in particle size. There is in particular a considerable particle size difference between the small-particle Si-MCM(S) sample and the large-particle

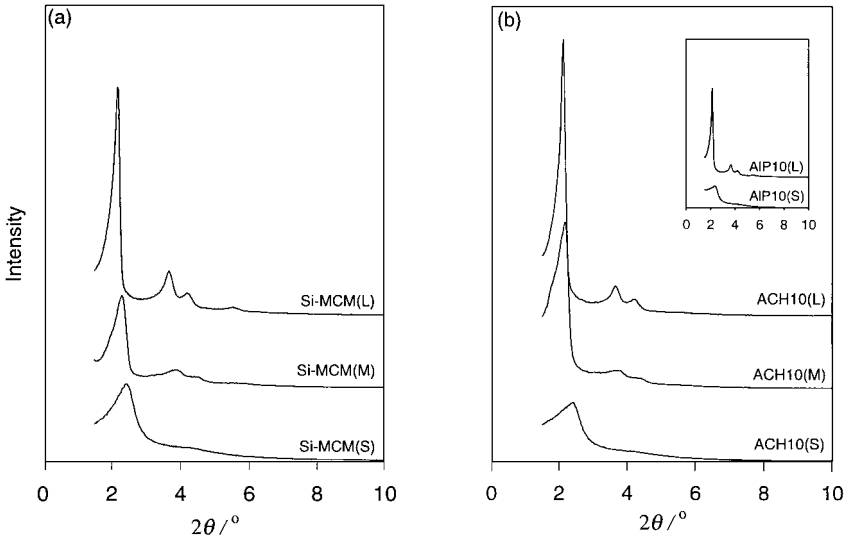

FIG. 1. Powder XRD patterns of calcined (a) purely siliceous and (b) Al-grafted MCM-41 samples. L, M, and S indicate large-, medium-, and small-particle samples, respectively.

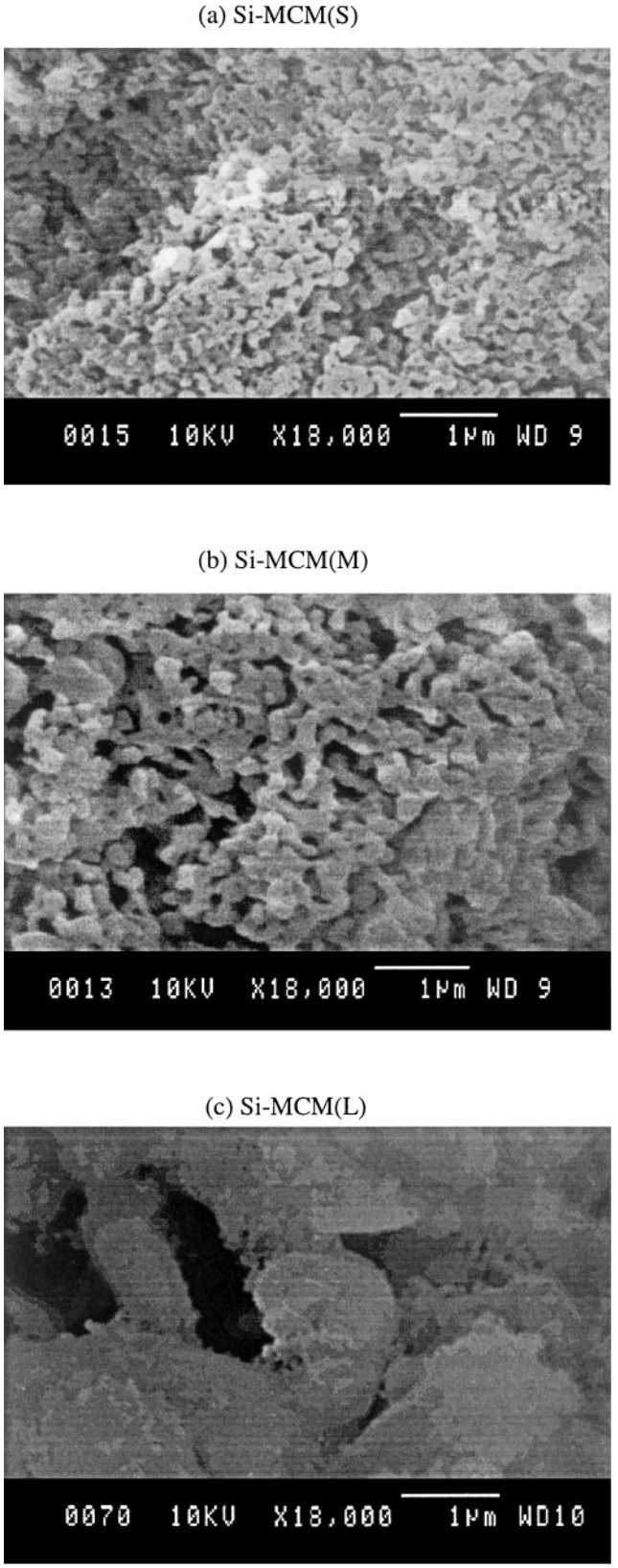

FIG. 2. SEM images of pure silica MCM-41 of varying particle size: (a) small particle, Si-MCM(S); (b) medium particle, Si-MCM(M); and (c) large particle, Si-MCM(L) (bar at the bottom of each micrograph, 1 μm).

Si-MCM(L) sample; for this reason most of the comparisons in this report are between these two samples. It is worth noting that the particle size variations observed here may be accompanied by changes in the level of silicate condensation (and therefore population of silanol groups), which may also affect the grafting process. Indeed ^{29}Si NMR and XRD (i.e., the extent of lattice contraction on calcination) indicated that the level (or extent) of silicate condensation in the as-synthesised Si-MCM samples increased with particle size; for example, on calcination the contraction in the d_{100} spacing was 18.4, 8.3, and 4.8% for Si-MCM(S), Si-MCM(M), and Si-MCM(L), respectively. Therefore in the as-synthesised samples, the population of silanol groups decreases as the particle size increases. However, critical to the study reported here is the fact that calcination removed the differences in the extent of silicate condensation—^{29}Si NMR indicated similar Q^4/Q^3 ratios for the calcined samples and therefore the population of silanol groups was disregarded as an influencing factor in the grafting process.

Chemical Composition of Al-Grafted Materials

Elemental compositions of the Al-grafted materials, given as bulk Si/Al ratio, are shown in Table 1. In all cases the Si/Al molar ratios obtained are close to the target Si/Al ratio of 10, indicating that particle size has little or no effect on the uptake and retention of Al. In the present case it also means that differences in long-range structural ordering (see Fig. 1a) do not affect the retention of Al in the parent Si-MCM materials. X-ray photoelectron spectroscopy was performed so as to determine the distribution of Al and also to characterise the Al species on the external surface of the Al-grafted samples. The surface Si/Al ratio and binding energies (BE) are given in Table 1. A comparison of the surface and bulk (or average) Si/Al ratio indicates that the surface/near surface region of the Al-grafted samples is Al-rich. This is consistent with the grafting procedure in which the Al is first in contact with the outer region of the particles of the parent Si-MCM materials before being transported into the bulk. A closer inspection of the bulk and surface Si/Al ratios reveals that the

TABLE 1

Bulk (Average) and Surface Si/Al Ratio and Binding Energies for Al-Grafted MCM-41 Samples

			Binding energies (eV)		
Sample	Si/Al_{Bulk}	Si/Al_{XPS}	Si(2*p*)	Al(2*p*)	O(1*s*)
ACH10(S)	9.8	6.8	103.0	74.8	533.0
ACH10(M)	9.7	6.0	102.7	74.6	532.5
ACH10(L)	9.8	5.7	103.2	75.1	532.5
AlP10(S)	11.2	7.5	102.9	74.5	533.0
AlP10(L)	9.8	5.5	102.9	74.5	532.8

"Al concentration gradient" (between the surface and the bulk concentration) is higher for nonaqueous grafted (AIP10) samples. For example, the surface concentration of Al in the nonaqueous grafted AIP10(S) and AIP10(L) is 44 and 68% higher than the bulk concentration while for (the equivalent) ACH10(S) and ACH10(L) samples it is higher by 39 and 63%, respectively. This may be an indication that grafting in aqueous medium affords aluminosilicate materials with a slightly more uniform distribution of Al compared to grafting in nonaqueous medium. The XPS results also reveal that for both sets of materials, the Al concentration gradient increases with particle size. For ACH10 samples the surface Al concentration is higher than the bulk concentration by 39, 54, and 63% for small-, medium-, and large-particle samples, respectively. For AIP10 samples the corresponding values are 44% for small-particle samples increasing to 68% for the large-particle sample. The grafted Al is therefore better distributed into small particles than into larger particles. This indicates that the grafting process is, to some extent, diffusion controlled; presumably the interior of a large particle is less easily accessed by the guest Al because it is much further away than in a small particle.

The BE are also influenced by particle size since the Si 2*p* and O 1*s* BE do not as expected (in the absence of particle size differences) increase with increasing surface Si/Al ratio (27). Indeed despite a lower surface Si/Al ratio, the large-particle ACH10(L) sample has higher Si 2*p* binding energy than the corresponding medium- (ACH10(M)) and small- (ACH10(S)) particle samples. A similar trend is observed for the nonaqueous grafted (AIP10) samples for which the small- and large-particle samples exhibit similar Si 2*p* binding energies despite a considerably lower surface Si/Al ratio for the large-particle sample. It is therefore reasonable to assume that the surface Al is probably more closely linked with the host silica framework in small-particle samples. The differences observed in the BE are, however, modest and therefore particle size does not radically alter the way in which the surface Al interacts with the silica framework.

^{27}Al MAS NMR was performed in order to ascertain the nature and environment of the grafted Al. As shown in Fig. 3 the materials contain both tetrahedrally coordinated (framework) and octahedrally coordinated (nonframework) Al with resonance at ca. 53.0 and 0 ppm, respectively. In all cases the majority of the Al is in tetrahedral positions. Particle size does not appear to affect the proportion of tetrahedrally coordinated Al in any consistent manner. The ratio of tetrahedral to octahedral Al is similar for ACH10 samples while for AIP10 samples, the large particle sample has proportionately more octahedral Al; this may, however, be simply a consequence of its higher Al content (16, 17). The NMR results therefore suggest that the higher concentration of surface Al in large-particle samples does not necessarily indicate greater amounts of nonframework (octahedrally coordinated) Al. The picture that emerges from the foregoing chemical composition studies is that particle size does affect the distribution of Al but exerts lesser influence on the nature or environment of the Al once it is incorporated.

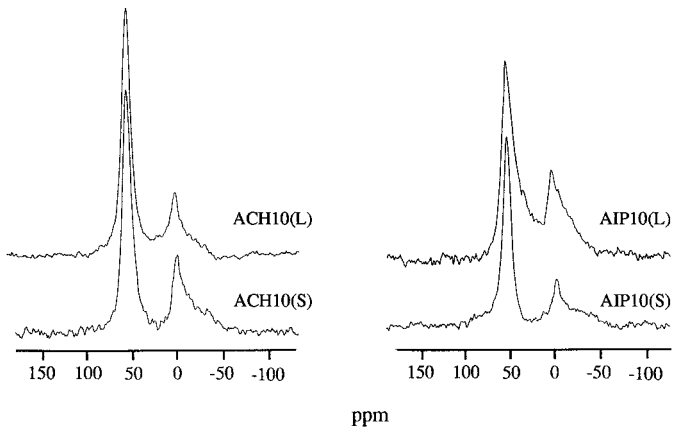

FIG. 3. ^{27}Al MAS NMR spectra of calcined Al-grafted MCM-41 samples.

Physical Characterisation

Figure 1b shows the powder X-ray diffraction patterns of the Al-grafted samples. The patterns are comparable to those of the parent Si-MCM, which is an indication that structural ordering is generally well maintained after Al insertion. In particular, the XRD patterns of the large- and medium-particle materials remain virtually unaffected. However, for the small-particle samples there is some significant reduction in the intensity of the (100) peak—compare Si-MCM(S) with ACH10(S) and AIP10(S) in Figs. 1b and 1b, inset. It appears therefore that the small-particle sample is more susceptible to structural degradation as a result of the insertion of Al. This may be related to the extent to which the Al is "sorbed" into the interior of the particles. Indeed the XPS data discussed above suggest that the Al penetrates the small particles to a greater extent. This means that particle size (and long-range ordering) plays a part in determining whether or not structural integrity is retained; the larger the particles the better the retention of structural ordering. It is therefore possible, by careful choice of the parent pure silica material, to prepare aluminosilicate MCM-41 with long-, medium-, or short-range structural ordering corresponding to long, medium, or short pores.

The retention (or not) of structural integrity is confirmed by the nitrogen sorption isotherms for the parent Si-MCM materials and the Al-grafted derivatives shown in Fig. 4. Note the difference in long-range pore uniformity between Si-MCM(S) and Si-MCM(L) that is clearly evident from the isotherms. Si-MCM(L) exhibits an isotherm

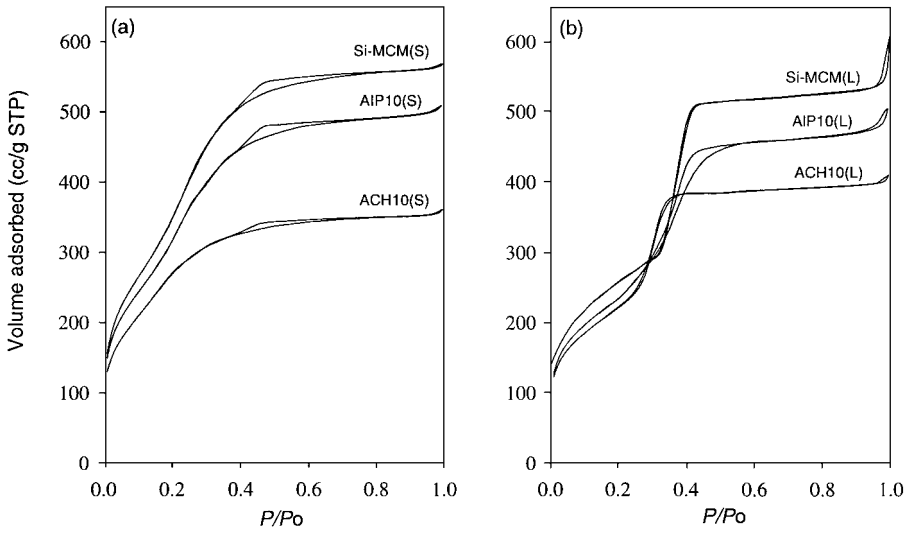

FIG. 4. Nitrogen sorption isotherms of (a) small-particle and (b) large-particle pure silica (top isotherm) and Al-grafted MCM-41 samples.

with a much better developed step in the relative pressure (P/P_o) range 0.3–0.45, characteristic of capillary condensation (filling) into uniform mesopores (28, 29). In both cases illustrated in Fig. 4 the sorption isotherms of the Al-grafted materials are (except for ACH10(s)) comparable to those of the parent PS materials. In particular, Al-grafted materials derived from the large-particle Si-MCM(L) (Fig. 4b) exhibit isotherms that retain the sharp well-developed mesopore filling step in the relative pressure (P/P_o) range 0.30 to 0.45, which is typical of well-ordered MCM-41 (28, 29). For both large-particle samples (ACH10(L) and AIP10(L)) the uniformity of the pores is therefore largely unaffected by Al insertion. For small-particle samples (especially for ACH10(S)), the height and steepness of the mesopore filling step is reduced to a greater extent than in the large-particle samples. The information derived from the isotherms is therefore in agreement with the XRD patterns (see Fig. 1) and points to excellent retention in structural ordering for large-particle samples while small-particle samples undergo some disruption of pore uniformity. Table 2 shows the textural properties for the parent Si-MCM materials and the corresponding Al-grafted materials. Consistent with the presence of tetrahedral Al in the framework, the basal d_{100} spacing increases (16, 17). The wall thickness of all the Al-grafted samples is also higher than that of the corresponding parent Si-MCM material, which is consistent with the incorporation of Al into the framework. In general (and regardless of the parent material) Al insertion leads to a decrease in the surface area and pore volume. The thicker walls of Al-grafted materials are partly reponsible for the lower surface area and pore volume. In agreement with the XRD and nitrogen sorption isotherms, the surface area and pore volume of the small-particle samples are reduced to a greater extent.

Acidity and Catalytic Activity

Table 3 gives the acid content of the Al-grafted materials obtained using thermally programmed desorption of cyclohexylamine (23–25). The procedure used to determine the acid content measured either the total acid content (pretreatment at 80°C) or the population of (medium to strong) acid sites that are sufficiently strong to retain the base after heat treatment at 250°C (11, 25). It is worth noting that under these measurement conditions, the purely siliceous (Si-MCM) material does not exhibit any acidity. From Table 3 it is clear that for both sets of samples, acidity is slightly higher for the small-particle samples. This is true for both total acid content and the content of medium to strong acid sites. This trend may be related to the

TABLE 2

Textural Properties of Pure Silica and Al-Grafted MCM-41 Materials of Varying Particle Size

Sample	Si/Al	d_{100} (Å)	Surface area (m^2/g)	Pore volume (cm^3/g)	APD (Å)	a_o (Å)	Wall thickness (Å)
Si-MCM(S)		33.8	1110	0.93	26.3	39.0	12.7
ACH10 (S)	9.8	35.6	859	0.55	25.3	41.1	15.8
AlP10(S)	11.2	36.0	996	0.78	26.6	41.6	14.9
Si-MCM(M)		38.6	949	0.94	30.5	44.6	14.1
ACH10(M)	9.7	40.8	801	0.75	28.9	47.1	18.2
Si-MCM(L)		41.2	887	0.85	31.6	47.6	16.0
ACH10(L)	9.8	42.0	760	0.69	29.3	48.5	19.2
AlP10(L)	9.8	41.4	850	0.76	30.9	47.8	16.9

Note. APD, average pore diameter (determined using BJH analysis).
a_o, the unit cell parameter, from the XRD data using the formula $a_o = 2d_{100}/\sqrt{3}$.

TABLE 3

Acidity and Catalytic Activity of Al-Grafted MCM-41 Materials

Sample	Acidity (μmol H^+/g)		Cumene conversion	
	80°C	250°C	Initial rate[a]	TOF
ACH10(S)	880	520	1172	2.25[b] (1.12)[c]
ACH10(M)	850	495	895	1.81
ACH10(L)	820	470	516	1.10 (0.45)
AlP10(S)	807	480	1120	2.33 (1.15)
AlP10(L)	633	440	704	1.60 (0.75)

[a] Obtained after 10 min on stream in μmol $(g \cdot cat \cdot h)^{-1}$.

[b] Obtained by dividing initial rate by the content of medium and strong acid sites (i.e., at 250°C).

[c] Obtained by dividing initial rate by the tetrahedral Al content (calculated from the ^{27}Al NMR and elemental composition).

presence of larger amounts of nonacidic surface Al in the large-particle samples. A comparison of the total acid content (after heat treatment at 80°C) with the concentration of tetrahedral Al (calculated from the ^{27}Al NMR and elemental composition) indicates that not all tetrahedral Al sites give rise to measurable acid sites. This comparison also reveals that the proportion of tetrahedral Al sites giving rise to acid sites is higher for small-particle samples. For ACH10(S) and AIP10(S) the percentage of Al sites giving rise to acid sites is 84 and 83%, respectively, while for ACH10(L) and AIP10(L) it is lower, at 72 and 67%, respectively. Since the total Al content is very similar in all the samples, this therefore means that the proportion of Al giving rise to acid sites is higher for small-particle materials, which is consistent with the XPS data. The ratio of acid content at 250°C to total acid content (at 80°C) indicates that there is no influence of particle size on the proportion of weaker acid sites; therefore particle size has no effect on the strength of acid sites.

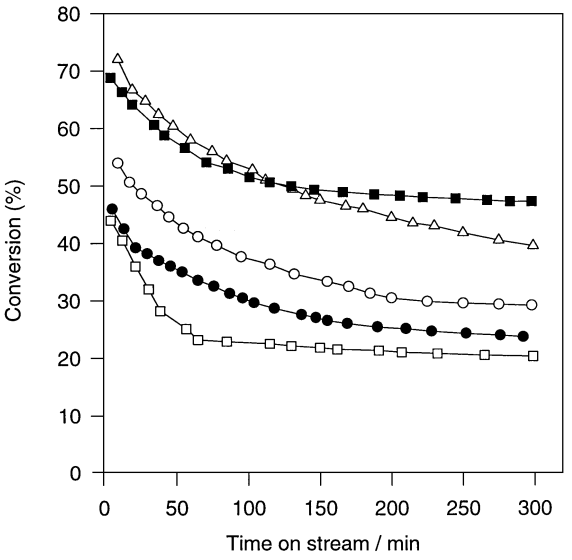

FIG. 5. Activity and deactivation behaviour during cumene conversion over Al-grafted samples of varying particle size compared at 300°C and WHSV of 5.5. ACH10(S) (△), ACH10(M) (○), ACH10(L) (□), AlP10(S) (■), and AIP10(L) (●).

The catalytic activity of the Al-grafted materials was evaluated using the conversion of cumene, which requires medium to strong acid sites (30). At 300°C the active sites are Brønsted acid sites and therefore the conversion proceeds almost exclusively via catalytic cracking to benzene and propene with only trace amounts of α-methylstyrene, the product of dehydrogenation over Lewis acid sites (30, 31). The results are given in Table 3 and Fig. 5. It is clear from the results that catalytic activity is higher for small-particle samples and decreases with an increase in particle size. The much higher activity of the small-particle samples cannot be explained by the modest differences in acidity alone. It is therefore likely that small particles offer other beneficial effects with respect to catalysis. One possibility is that the small particles with their shorter pores afford easier access to the active sites within their pores. In small particles the product molecules are also able to exit the short pores much more easily. If this were the case, the active sites on the small particles would turn out more product molecules per unit time. This is indeed the case as indicated by the TOF values given in Table 3 that confirm that activity per site is inversely proportional to particle size. Furthermore the trend in the TOFs calculated utilising the amount of tetrahedral Al reinforces this view. Since there is no evidence of stronger acid sites (which would increase TOF) on the small-particle samples, the only explanation for their higher TOF is their smaller particle size. This does not, however, mean that the reaction is diffusion controlled; the pore diameters are much too large for that to be the case. It is more likely related to the lower efficiency (e.g., longer transfer time) with which reactant and product molecules access or exit the long one-dimensional pores of the large particles. This explanation seems reasonable considering that the pores, with only two entry or exit points, can be as long as 800 nm (32). To confirm this phenomenon the effect of particle size on Al-grafted MCM-48 catalysts that have multidimensional pores is currently under way. The curves in Fig. 5 indicate that the rate and extent of deactivation are not influenced by particle size. For all samples deactivation occurs mainly during the first hour, after which relatively stable conversion levels are maintained. This confirms that the samples have acid sites of similar strength since differences in acid strength would have resulted in variations in rate and extent of deactivation (16, 17).

CONCLUSIONS

This report demonstrates that particle size (and therefore extent of long-range ordering) is an important factor

that influences both the preparation and the properties of Al-grafted MCM-41 catalysts. While particle size has little or no effect on the uptake and retention of Al, XPS studies show that it affects the distribution of Al, with larger particles having a higher concentration of outer surface Al. Small particles are "penetrated" by the guest Al to a much greater extent than large particles. However, the differences observed in the Si 2*p* binding energy as a function of particle size are modest, which means that particle size does not radically alter the way in which the surface Al interacts with the silica framework. Furthermore ^{27}Al MAS NMR indicates that particle size does not significantly affect the nature or environment of the Al once it is incorporated; the higher concentration of outer surface Al in large-particle samples does not translate to large amounts of nonframework (octahedrally coordinated) Al. Both XRD and porosity studies show that particle size plays a key role in determining whether or not structural integrity is retained after Al insertion. The surface area and pore volume of small-particle samples are reduced to a greater extent. Large-particle pure silica materials, which possess long-range ordering, are more likely to retain their structural ordering and textural properties after Al insertion. The acid content of small-particle samples is slightly higher than that of large-particle samples, presumably due to better Al insertion. The proportion of tetrahedral Al sites giving rise to acid sites is higher for small-particle samples. However, particle size has no effect on acid strength. Of particular significance is the observation that the catalytic activity of small-particle samples is much higher than that of large particles. The much higher activity of the small-particle (short pore) samples (which cannot be explained by the modest differences in acidity alone) is ascribed to the higher efficiency with which reactant and product molecules access or exit their shorter pores. The molecule transfer efficiency is expected to be significantly lower in the much longer one-dimensional pores of the large particles.

ACKNOWLEDGMENT

The author is grateful to the EPSRC for an Advanced Fellowship.

REFERENCES

1. Biz, S., and Occelli, M. L., *Catal. Rev. Sci. Eng*. **40**, 329 (1998).
2. Corma, A., *Chem. Rev*. **97**, 2373 (1997).
3. Sayari, A., *Chem. Mater*. **8**, 1840 (1996).
4. Corma, A., Fornés, V., Navarro, M. T., and Pérez-Pariente, J., *J. Catal*. **148**, 569 (1994).
5. Mokaya, R., Jones, W., Luan, Z., Alba, M. D., and Klinowski, J., *Catal. Lett*. **37**, 113 (1996).
6. Reddy, K. M., Moudrakovski, I., and Sayari, A., *J. Chem. Soc. Chem. Commun*. 1059 (1994).
7. Corma, A., Navarro, M. T., and Pérez-Pariente, J., *J. Chem. Soc. Chem. Commun*. 147 (1994).
8. Zhao, D., and Goldfarb, D., *J. Chem. Soc. Chem. Commun*. 875 (1995).
9. Yuan, Z. Y., Liu, S. Q., Chen, T. H., Wang, J. Z., and Li, H. X., *J. Chem. Soc. Chem. Commun*. 973 (1995).
10. Sayari, A., Danumah, C., and Moudrakovski, I. L., *Chem. Mater*. **7**, 813 (1995).
11. Mokaya, R., and Jones, W., *J. Catal*. **172**, 211 (1997).
12. Mokaya, R., and Jones, W., *Chem. Commun*. 2185 (1997).
13. Ryoo, R., Jun, S., Kim, J. M., and Kim, M. J., *Chem. Commun*. 2225 (1997).
14. Maschmeyer, T., Rey, F., Sankar, G., and Thomas, J. M., *Nature* **378**, 159 (1995).
15. Mehnert, C. P., and Ying, J. Y., *Chem. Commun*. 2215 (1997).
16. Mokaya, R., and Jones, W., *Phys. Chem. Chem. Phys*. **1**, 207 (1999).
17. Mokaya, R., and Jones, W., *J. Mater. Chem*. **9**, 555 (1999).
18. Chen, C. Y., Li, H-X., and Davis, M. E., *Microporous Mater*. **2**, 17 (1993).
19. Mokaya, R., and Jones, W., *Chem. Commun*. 1839 (1998).
20. Ray, G. J., Meyes, B. L., and Marshall, C. L., *Zeolites* **7**, 307 (1987).
21. Man, P. P., Klinowski, J., Trokiner, A., Zanni, H., and Papon, P., *Chem. Phys. Lett*. **151**, 143 (1988).
22. Grabowski, R., Grzybowska, B., Samson, K., Sloczynski, J., Stoch, J., and Wcislo, K., *Appl. Catal. A*. **125**, 129 (1995).
23. Ballantine, J. A., Purnell, J. H., and Thomas, J. M., *Clay Miner*. **18**, 347 (1983).
24. Breen, C., *Clay Miner*. **26**, 487 (1991).
25. Mokaya, R., Jones, W., Moreno, S., and Poncelet, G., *Catal. Lett*. **49**, 87 (1997).
26. Tanev, P. T., and Pinnavaia, T. J., *Chem. Mater*. **8**, 2068 (1996).
27. He, H., Cheng, C. F., Seal, S., Barr, T. L., and Klinowski, J., *J. Phys. Chem*. **99**, 3235 (1995).
28. Branton, P. J., Hall, P. G., Sing, K. S. W., Reichert, H., Schüth, F., and Unger, K. K., *J. Chem. Soc. Faraday Trans*. **90**, 2965 (1994).
29. Rathousky, J., Zukal, A., Franke, O., and Shulz-Ekloff, G., *J. Chem. Soc. Faraday Trans*. **90**, 2821 (1994).
30. Mokaya, R., and Jones, W., *J. Catal*. **153**, 76 (1995).
31. Ward, J. W., *J. Catal*. **9**, 225 (1967); **11**, 251, 259 (1968).
32. Mokaya, R., Zhou, W., and Jones, W., *Chem. Commun*. 51 (1999).